

Automated Detection And Classification Of Pneumonia And Tuberculosis Using Chest X-Ray Images

Vividha¹, Naman Chawla², Soham Taneja³, Preeti Nagrath⁴, Rachna Jain⁵, Narina Thakur⁶

^{1, 3, 4} *Bharati Vidyapeeth’s College Of Engineering, New Delhi*

^{2, 6} *Department of Computer Science and Engineering, Bhagwan Parshuram Institute of Technology, Delhi*

⁵ *Department of Information technology, Bhagwan Parshuram Institute of Technology, Delhi*

1vividha.cse1@bvp.edu.in , 2naman89ceeb21@bpitindia.edu.in , 3sohamtaneja.cse1@bvp.edu.in ,
4preeti.nagrath@bharatividyapeeth.edu , 5rachnajain@bpitindia.com , 6narinat@gmail.com

Abstract—*Pneumonia and tuberculosis are leading causes of death in children and the elderly. Furthermore, the fact that despite being curable with proper treatment the numbers of deaths by these diseases is high. In a country with such a large population, the smaller number of doctors is a problem due to which the diagnosis of these diseases is not that accurate and often flawed. Our research proposes a deep learning-based model to classify and detect pneumonia and tuberculosis using Convolutional Neural Networks. The dataset used for Pneumonia consists of chest x-rays of 1 - 5 years of age from Guangzhou women and children’s medical center, Guangzhou, consisting of 5,863 images and for tuberculosis contains 662 chest x-rays. Our model detected pneumonia with an accuracy and recall percentage of 91% while the accuracy achieved in detecting tuberculosis is 87% with a recall percentage of 88%.*

Keywords- *Machine Learning, Deep Learning, Convolutional Neural Network, Max Pooling, Kernel*

I. INTRODUCTION

Pneumonia has been one of the most common and deadliest diseases throughout the history of mankind. Globally around 450+ million people are affected by pneumonia resulting in about four million deaths per year [1, 2, 3]. Pneumonia results in inflamed lungs, which is caused by microorganisms, such as viruses, bacteria and fungi[4], which may become life-threatening for infants and children, people having low immune system, elderly people and people who have adverse lifestyle like smoking cigarettes [5,6]. Based on its because there are primarily three variants of pneumonia: Viral pneumonia, Bacterial pneumonia and Fungi pneumonia. Pneumonia caused by viruses is less harmful as compared to pneumonia caused by bacteria [7]. However, it becomes difficult to differentiate between the two. India being a developing nation is about five times more frequent in these cases than the other developing nations [1]. UNICEF in its recent survey and assessment ranked India second in terms of number of people passing because of pneumonia. Most of these deaths took place among children under the age of two and the fact that it is a curable and preventable disease makes it even more alarming [8]. Another such disease is Tuberculosis. As of 2018 around 25% of the world’s population is affected by Tuberculosis [9]. Globally, in 2017 there have been more than 10 million diagnosed TB cases out of which 1.6 million resulted in death which made it

the infectious disease resulting into most number of deaths [10]. Tuberculosis is generally affects the lungs of the person and spreads through air [11, 12]. In India, nearly 200,000+ deaths from Tuberculosis are reported annually [13]. According to World Health Organization, India faces the largest burden of TB worldwide with statistics of 2011 to offer an approximate incidence of 2.2 million TB cases in India out of 9.6 million cases reported globally [14,15]. Therefore, an accurate prognosis of such diseases is very crucial and fundamental in order to provide a timely treatment to those needed. But in a country with ever increasing population and limited doctors it is difficult to achieve this. With the recent advancements in Deep Learning, Convolutional Neural Networks could be used to determine the presence of disease using the dataset of X-ray images of patients suffering from pneumonia and tuberculosis and also classify its type [16]. For instance, in cases of pneumonia like a doctor analyzes the X-Ray images by identifying the white patches in the lungs, similarly CNN uses feature extraction layer by layer to detect pneumonia. The objective of this research is to provide an automated diagnosis of pneumonia and tuberculosis using Chest Radiography and classify its types using Deep Learning Methodologies. The paper is segregated into seven sections. The first section gives the Introduction of the problem at hand. The next section discusses the related work on the topic, identifying the gaps in the literature. The third section describes the Materials and Methods which includes the description of dataset, input structure, convolutional layer and pooling layer. The fourth section talks about the various metrics of evaluation used in deep learning like confusion matrix and ROC curve. The fifth section comprises of the results and brief discussion of the same. The sixth section is a comparison analysis of the paper. Finally the conclusion has been drawn in the last section summarizing the research work and results and findings.

II. RELATED WORK

Chest radiographs generally present for a variety of manifestations, including arteries, focal lesions, opacity joint and ears that add to the problems of diagnosing TB alone. The first proposed approaches for automatic TB diagnosis is the local texture of CXRs to get a contrasting touch, were extracted and studied in [17]. The winged areas are split into multi-point zones. The nearest K neighbor was then used at the district level to conduct classic operations. For example, Wang et al., proposed a new dataset named Chest X-ray 8 [18] that consisted of images of 32,717 unique patients, whose 108,948 frontal X-ray images were obtained. With this dataset they were able to attain favorable results using CNN with deep network. Furthermore, they declared that the dataset is expandable by increasing the disease labels. The authors have achieved significant accuracy, even upon training small batches of images using data augmentation techniques in addition to CNN [19].

In a separate study, the authors explained how deep CNNs can be leveraged for detecting lymph nodes [20]. They achieved assuring results despite poor image quality [21] Worked in CNN's architecture and solved the problem of lung disease diagnosis. The study of [22] aims to visualize the high-performance network in a model based on CNN, which is used for the chest X-ray examination. Using machine learning algorithms, computer-aided software's were created to study CXRs with anomalies so as to reduce delays and limited resources. A CNN based [23] technique, was conjugate with lung field segmentation and rib suppression. For the pixel spots fetched from the lung region, 3 different CNN models were trained using images with varying resolution. Feature fusion method was used to concatenate the entire

information obtained [24]. A curated network which was created using 49 different convolutional layers was proposed in [25]. In addition to the CNN layers, 1 average pooling layer and 2 fully connected dense layers were used to detect pneumonia. It uses a 25-layer, deep CNN with eight residual connections [26]. Authors have proposed two architectures of the 3D specialized mixed connection network (CMixNet). Recognition of the lung nodule was carried out with faster RCNN. Authors of [27] have proposed a custom neural network which was made using 5 different CNN blocks (each with 2 (3,3) convolutions with Rectified Linear Units (ReLU), which was succeeded by an average pooling layer and a dense layer with 2 outputs activated with softmax function.

Authors have proposed a CNN model which was based on AlexNet for lung patch detection tasks [28]. Further, a 2nd CNN model using ResNet18 as a backbone was created to remodel the lacking blocks in the lung area. The output was fetched by the ensemble model created using the initial segmentation and reconstruction. Researchers have utilized the state-of-the-art network architectures such ResNet, VGG16/19 [29], and Inception etc., modified and experimented with the pooling and flattening functions. Final the results were fetched by dense layers activated using the sigmoid function. Along with this, CNNs tend to perform optimally on fairly large datasets but most of the time; it produces incorrect outputs on small datasets.

III. MATERIALS AND METHODS

This section discusses dataset and various classification techniques, CNN architectures as shown in Fig6 and Fig7, methodology and evaluation metric employed.

A. Description of the Dataset

- **Pneumonia**

The dataset includes anteroposterior chest radiographs obtained from pediatrics in the age band of 1 to 5 years from Guangzhou women and children's medical center, Guangzhou [30]. The chest radiographs are obtained during the clinical medical tests of the patients suffering from pneumonia or having symptoms of pneumonia as shown in Fig1.



Fig 1: Chest X ray images indicating the following (a) Normal (b) Bacterial Pneumonia (c) Viral Pneumonia

The data is organized into three folders: training, testing, and validation, with references to each of the four image categories (Pneumonia / General). There are over 5,800 JPEG X-Ray images and two phases (Pneumonia / Normal) [31]. For the study of x-ray images, originally, all x-rays were checked for quality control. Before being cleared to be used as a dataset for our deep learning model, the

diagnoses for the images were graded by two expert physicians. In case of grading errors, the test set was also double-checked by a third expert. In case of pneumonia, the alveoli get filled with a secreted liquid and are visible as a white patch on the x-ray image. This condition is known as pulmonary consolidation where pulmonary alveoli are filled with inflammatory liquid. In radiography, the whitish area or the opacity corresponds to the pulmonary consolidation which is one of main features in detection of pneumonia [32].

- **Tuberculosis**

The dataset used for training the model of tuberculosis included over 500 X-Rays images with 336 cases of tuberculosis in addition to 326 normal cases, which were collected from the “National Library of Medicine, National Institutes of Health, Bethesda, MD, USA and Shenzhen No.3 People’s Hospital, Guangdong Medical College, Shenzhen, China” [33]. The data set also contains radiology data, which is provided in the form of a text file.

B. Methodology

- **Input Structure**

The input image is fed to the proposed model which classifies the input image into two classes - Normal or Pneumonia. Images are converted to grayscale and normalized between 0 and 1 as in Fig2.

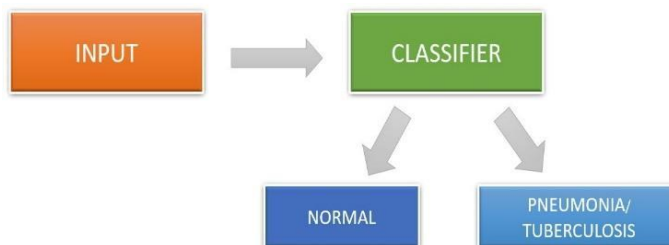


Fig 2: Classification Structure

- **Convolution Layers**

The model’s first layer is made up of the first two convolutional layers which do the main feature extraction and identification by using a filter [34] as in Fig4. Its filters are made up of an array with distinct values for the purpose of detecting the features. These filters move on all parts of the images and generate a high value if the feature is found. If the feature is not detected, then they generate a low value. To elaborate, the filters can be considered as a kernel of matrix consisting of distinct values [35]. The image is also a matrix of integer values which represent the intensity of the pixel present at that point, with values in the range: 0 – 255 [36, 37]. These kernels move from left to right as well as top to bottom.

While doing so, they multiply the kernel values with the pixels in the image matrix and the total of all the values is recorded in the output matrix. Doing so aids to extract features from the given image. For the model used in this paper, a (3, 3) size kernel

was considered to be used experimentally, as it provided higher accuracy in the time required to traverse the whole image as in Fig 3.

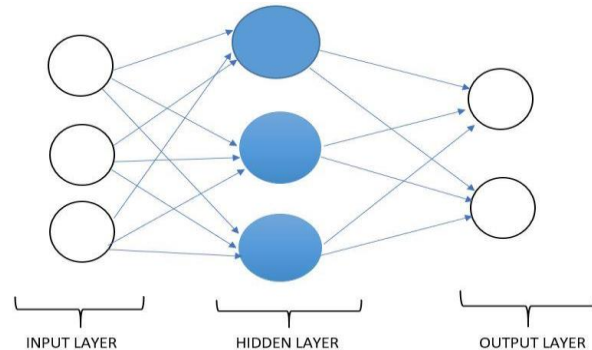


Fig3: Neural Network Structure

$$G[m, n] = (f * h)[m, n] = \sum \sum h[j, k] f[m - j, n - k] \quad (1)$$

Subsequent map values are determined using the formula given above, where the input image is denoted by f and our kernel is denoted by h . The result matrix rows and column indexes are labelled with m and n , respectively.

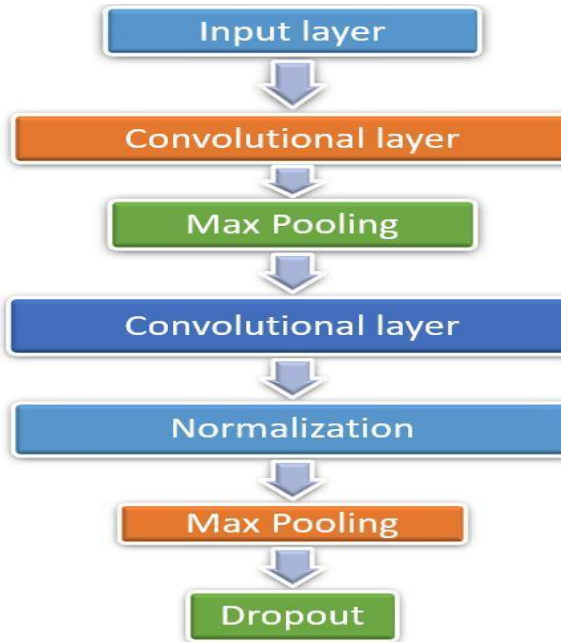


Fig 4: Model Architecture consisting of different layers of operation

C. Max Pooling

After convolutional layers, we used a Max-pool layer as in Fig5. The Pooling layer is the same as the Convolutional layer. It is used to reduce the spatial scale of the expressed feature. It also helps to reduce the training time as well as avoids overfitting [38]. It reduces the computational power for data processing by reducing the dimensionality [39]. In addition, it prevents overfitting by extracting dominant positional and rotational invariant features.

Pooling is of two types. First Average Pooling where an average of all values from the kernel covered portion of the image is returned.

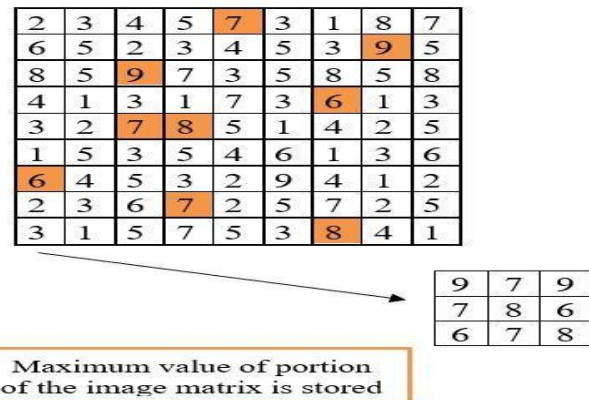


Fig 5: Example of Max pooling with 9x9 image

Second Max Pooling as the name suggests returns the maximum value of all the values covered by the kernel image portion. Max pooling is better than average pooling as it also acts as Noise Suppressant along with dimensionality reduction [40]. The model used in this research has used max pooling.

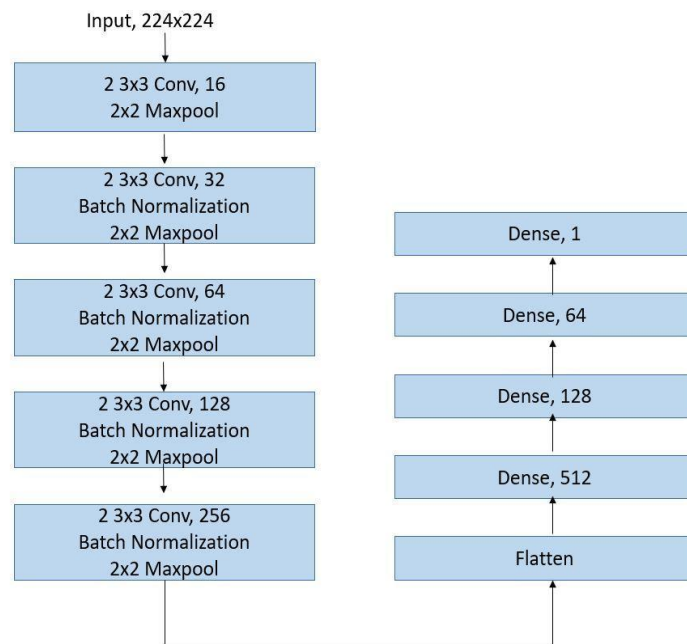


Fig 6: CNN Architecture for Pneumonia

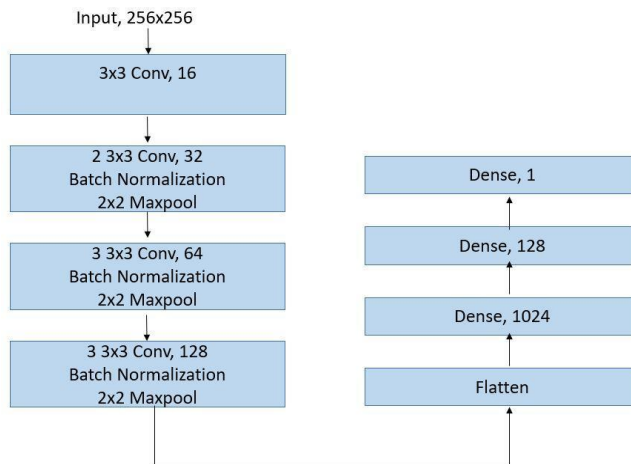


Fig 7: CNN Architecture for Tuberculosis

D. Evaluation metrics

- **Confusion Matrix**

A matrix consisting of accurate and erroneous predictions of the model and the original labels is known as the Confusion Matrix [41].

- True Positive: Number of people who suffer from pneumonia as predicted by the model.
- False Negative: Number of people who are infected with pneumonia but are predicted healthy by the model.
- False Positive: Number of people not actually infected but predicted as pneumonia-affected, by the model.
- True Negative: Number of people whose x-ray is normal and the model predicted them as normal.

- **ROC Curve**

The Receiver Operating Characteristic Curve or ROC curve is a graphical image that is used to represent the relationship between the true positive value and the false positive value under the limit of different decisions. The true positive rate is the recall or probability of classification. The ROC curve is an important metric of evaluation in determining the reliability of diagnostic tests [42]. The analysis by ROC curve helps in optimization of the model by providing tools to select the most fitting model. It can be described as a straight way to benefit the decision making process of the model. It is the most used metric in the machine learning community [43].

- **Precision, Recall and f1-score**

In classification, precision is part of the optimal conditions between the obtained conditions as in (2), and the recall is part of the total number of correct conditions actually obtained as in (3). Thus, both precision and recall are based on measurement and perceptual processing. F1 score is the measure of a test's accuracy as in (4) [44].

$$Precision = \frac{TP}{TP+FP} \quad (2)$$

$$Recall = \frac{TP}{TP+FN} \quad (3)$$

$$f1-score = \frac{2 \times Precision \times Recall}{Precision+Recall} \quad (4)$$

Where TP is True Positive, FN is False Negative, FP is False Positive and TN is True Negative.

IV. RESULTS

This section contains the results of both proposed models to classify pneumonia and tuberculosis as in Table 1.

Table 1: Performance on Training, Validation and Test Data

Accuracy	Pneumonia	Tuberculosis
Training Data	94.5%	91.8%
Validation Data	93.12%	83.0%
Test Data	91.0%	84.0%

This paper utilizes the pre-trained models given below to classify X-rays [45]. First, the residual neural network (ResNet) has been employed. ResNet is a neural input network of the type that builds on counterflying cells. The residual neural networks do this by skipping connections, or shortcuts to get more into other layers. Standard ResNet models are used with double or triple skip with nonlinearities (ReLU) and batch normalization [46]. It's a convolutional neural network that is trained in over a million images from ImageNet data [47].

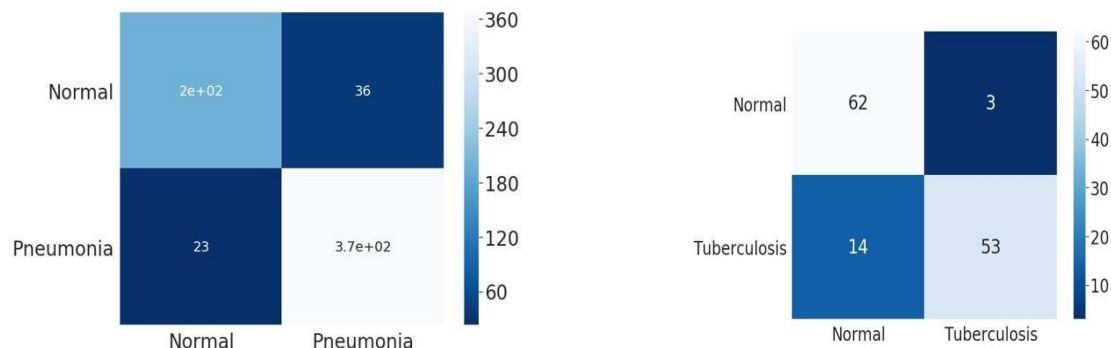


Fig 8: Confusion Matrix for (a) Pneumonia (b) Tuberculosis

A DenseNet which is also a convolutional neural network but with 201 layers whereas in Inception Resnet has been employed with 164 layers.

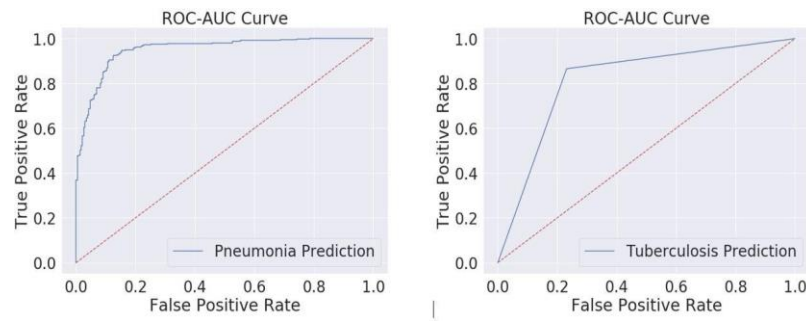


Fig 9: ROC Curve for (a) Pneumonia (b) Tuberculosis

	precision	recall	f1-score	support
0	0.90	0.85	0.87	234
1	0.91	0.94	0.93	390
accuracy			0.91	624
macro avg	0.90	0.89	0.90	624
weighted avg	0.91	0.91	0.90	624

	precision	recall	f1-score	support
0	0.82	0.97	0.89	65
1	0.96	0.79	0.87	67
accuracy			0.88	132
macro avg	0.89	0.88	0.88	132
weighted avg	0.89	0.88	0.88	132

Fig 10: Precision, Recall and f1-scores on Test Set of (a) Pneumonia (b) Tuberculosis

The ROC, Precision, Recall and f1-scores on Test Set for both Pneumonia and Tuberculosis are as in Fig 9 and Fig 10. Table 2 displays the results of these three pre-trained models on different datasets.

Table 2: Accuracy of the three pre-trained model

Pre-trained model	Internal Chest X-ray 14	Montgomery	Shenzhen
ResNet 152	0.8675	0.7005	0.7496
Inception-ResNet	0.9606	0.8552	0.9179
DenseNet121	0.9872	0.9139	0.9384

The DenseNet121 pre-trained deep learning model has ensured a dominant result in Pneumonia and Tuberculosis detection as compared to the other state-of-art Pre-trained models such as ResNet-152 and Inception-ResNet. Inception-ResNet also has performed well.

V. CONCLUSION

The research study presents two deep learning models to detect and classify pneumonia and tuberculosis using CNN. The proposed models for both pneumonia and tuberculosis gave noteworthy results with the accuracy for pneumonia being 91% and for the latter being 87%. The main aim of this research was the application of deep learning and machine learning in the healthcare sector. With the more advancement in future the models can be trained to classify many more diseases and help in various diagnoses with improved accuracy and precision. Other new architectures, such as EfficientNet and HR-Net, can also be used for future research.

REFERENCES

- [1]. Ruuskanen O, Lahti E, Jennings LC, Murdoch DR (April 2011). "Viral pneumonia". *Lancet.* 377 (9773): 1264–75.
- [2]. Lodha R, Kabra SK, Pandey RM (June 2013). "Antibiotics for community-acquired pneumonia in children". *The Cochrane Database of Systematic Reviews.* 6 (6)
- [3]. George, Ronald B. (2005). *Chest medicine: essentials of pulmonary and critical care medicine* (5th ed.). Philadelphia: Lippincott Williams & Wilkins. p. 353.
- [4]. McLuckie, A., ed. (2009). *Respiratory disease and its management*. New York: Springer. p. 51.
- [5]. Mandell LA, Wunderink RG, Anzueto A, Bartlett JG, Campbell GD, Dean NC, Dowell SF, File TM, Musher DM, Niederman MS, Torres A, Whitney CG (March 2007). "Infectious Diseases Society of America/American Thoracic Society consensus guidelines on the management of community-acquired pneumonia in adults". *Clinical Infectious Diseases.* 44 Suppl 2 (Suppl 2): S27–72.
- [6]. Lim WS, Baudouin SV, George RC, Hill AT, Jamieson C, Le Jeune I, Macfarlane JT, Read RC, Roberts HJ, Levy ML, Wani M, Woodhead MA (October 2009). "BTS guidelines for the management of community acquired pneumonia in adults: update 2009". *Thorax.* 64 Suppl 3 (Suppl 3): iii–155.
- [7]. Elena, Prina; Otavio, T Ranzani; Anthoni, Torres (12 August 2015). "Community-acquired pneumonia". *The Lancet.* 386 (9998): 1097–1108.
- [8]. Rudan I, Boschi-Pinto C, Bilooglav Z, Mulholland K, Campbell H (May 2008). "Epidemiology and etiology of childhood pneumonia". *Bulletin of the World Health Organization.* 86 (5): 408–16.
- [9]. WHO (June 1999). "Pneumococcal vaccines. WHO position paper". *Relevé Epidemiologique Hebdomadaire.* 74 (23): 177–83.
- [10]. Global tuberculosis report". World Health Organization (WHO). Retrieved 9 November 2017.
- [11]. Nicas M, Nazaroff WW, Hubbard A (March 2005). "Toward understanding the risk of secondary airborne infection: emission of respirable pathogens". *Journal of Occupational and Environmental Hygiene.* 2 (3): 143–54.

[12]. Dolin, [edited by] Gerald L. Mandell, John E. Bennett, Raphael (2010). Mandell, Douglas, and Bennett's principles and practice of infectious diseases (7th ed.). Philadelphia, PA: Churchill Livingstone/Elsevier. p. Chapter 250

[13]. TB Statistics for India. (2012). TB Facts. Retrieved April 3, 2013, from <http://www.tbifacts.org/tb-statistics-india.html>

[14]. "India records 2.15m new TB patients in 2018". The Nation. 2019-03-26. Retrieved 2019-03-27.

[15]. Sachdeva, Kuldeep Singh et al. "New vision for Revised National Tuberculosis Control Programme (RNTCP): Universal access - "reaching the un-reached".". The Indian journal of medical research vol. 135,5 (2012): 690-4.

[16]. Rajpurkar P, Irvin J, Zhu K, Yang B, Mehta H, Duan T, Ding D, Bagul A, Langlotz C, Shpanskaya K, Lungren MP (2017-11-14). "CheXNet: Radiologist-Level Pneumonia Detection on Chest X-Rays with Deep Learning"

[17]. Van Ginneken, B., Katsuragawa, S., ter Haar Romeny, B.M., Doi, K., Viergever, M.A.: Automatic detection of abnormalities in chest radiographs using local texture analysis. *IEEE Trans. Med. Imaging* 21(2), 139–149 (2002).

[18]. Wang, X.; Peng, Y.; Lu, L.; Lu, Z.; Bagheri, M.; summers, R.M. Chestx-ray8: Hospital scale chest x-ray database and benchmarks on weakly-supervised classification and localization of common thorax diseases. In *Proceedings of the IEEE Conference on Computer Vision and Pattern Recognition*, Honolulu, HI, USA, 21–26 July 2017; IEEE: Piscataway, NJ, USA; pp. 2097–2106.

[19]. Ronneberger, O.; Fischer, P.; Brox, T. U-net: Convolutional networks for biomedical image segmentation. In *Proceedings of the 18th International Conference on Medical Image Computing and Computer-Assisted Intervention*, Munich, Germany, 5–9 October 2015; Springer International Publishing: New York, NY, USA; pp. 234–241.

[20]. Roth, H.R.; Lu, L.; Seff, A.; Cherry, K.M.; Hoffman, J.; Wang, S.; Liu, J.; Turkbey, E.; Summers, R.M. A new 2.5 d representation for lymph node detection using random sets of deep convolutional neural network observations. In *Proceedings of the 17th International Conference on Medical Image Computing and Computer-Assisted Intervention*, Boston, MA, USA, 14–18 September 2014; Springer International Publishing: New York, NY, USA; pp. 520–527.

[21]. Shin, H.-C.; Roth, H.R.; Gao, M.; Lu, L.; Xu, Z.; Nogues, I.; Yao, J.; Mollura, D.; Summers, R.M. Deep convolutional neural networks for computer-aided detection: Cnn architectures, dataset characteristics and transfer learning. *IEEE Trans. Med. Imaging* 2016, 35, 1285–1298.

[22]. Sivaramakrishnan, R., Antani, S., Xue, Z., Candemir, S., Jaeger, S., and Thoma, G. (2017). Visualizing abnormalities in chest radiographs through salient network activations in deep learning. In *Life Sciences Conference (LSC), 2017 IEEE*, pages 71–74. IEEE.

[23]. Li, X.; Shen, L.; Xie, X.; Huang, S.; Xie, Z.; Hong, X.; Yu, J. Multi-resolution convolutional networks for chest X-ray radiograph based lung nodule detection. *Artif. Intell. Med.* 2019, 101744.

[24]. Liang, G.; Zheng, L. A transfer learning method with deep residual network for pediatric pneumonia diagnosis. *Comput. Methods Programs Biomed.* 2019, 104964.

[25]. Nam, J.G.; Park, S.; Hwang, E.J.; Lee, J.H.; Jin, K.; Lim, K.Y.; Park, C.M. Development and validation of deep learning-based automatic detection algorithm for malignant pulmonary nodules on chest radiographs. *Radiology* 2019, 290, 218–228.

[26].. Nasrullah, N.; Sang, J.; Alam, M.S.; Mateen, M.; Cai, B.; Hu, H. Automated lung nodule detection and classification using deep learning combined with multiple strategies. *Sensors* 2019, 19, 3722.

[27]. Pasa, F.; Golkov, V.; Pfeiffer, F.; Cremers, D.; Pfeiffer, D. Efficient deep network architectures for fast chest X-ray tuberculosis screening and visualization. *Sci. Rep.* 2019, 9, 6268.

[28]. Souza, J.C.; Bandeira Diniz, J.O.; Ferreira, J.L.; França da Silva, G.L.; Corrêa Silva, A.; de Paiva, A.C. An automatic method for lung segmentation and reconstruction in chest X-ray using deep neural networks. *Comput. Methods Programs Biomed.* 2019, 177, 285–296.

[29]. Taylor, A.G.; Mielke, C.; Mongan, J. Automated detection of moderate and large pneumothorax on frontal chest X-rays using deep convolutional neural networks: A retrospective study. *PLoS* ed. 2018, 15,e1002697.

[30]. Daniel Kermany, Kang Zhang, Michael Goldbaum Labeled Optical Coherence Tomography (OCT) and Chest X-Ray Images for Classification

[31]. Kermany, D., Zhang, K., and Goldbaum, M. (2018). Labeled optical coherence tomography (oct) and chest x-ray images for classification. *Structural Equation Modeling: A Multidisciplinary Journal*.

[32]. Sharma S, Maycher B, Eschun G (May 2007). "Radiological imaging in pneumonia: recent innovations". *Current Opinion in Pulmonary Medicine*. 13 (3): 159–69.

[33]. Johnson AEW, Pollard TJ, Berkowitz SJ, Greenbaum NR, Lungren MP, Deng CY, Mark RG, Horng S. MIMIC-CXR, a de-identified publicly available database of chest radiographs with free-text reports. *Sci Data*. 2019 Dec 12;6 (1):317.

[34]. Ustinova, E., Ganin, Y., and Lempitsky, V. (2017). Multiregion bilinear convolutional neural networks for person re-identification. In *Advanced Video and Signal Based Surveillance (AVSS)*, 2017 14th IEEE International Conference on, pages 1–6. IEEE.

[35]. Albawi, S.; Mohammed, T.A.; Al-Zawi, S. Understanding of a convolutional neural network. In *Proceedings of the 2017 International Conference on Engineering and Technology (ICET)*, Antalya, Turkey, 21–23 August 2017; pp. 1–6.

[36]. Gomes, J.; Velho, L. *Image Processing for Computer Graphics and Vision*. Springer-Verlag, 2008.

[37]. Gonzalez, R. C.; Woods, R. E. *Digital Image Processing*. Third Edition. Prentice Hall, 2007.

[38]. Yu, S., Jia, S., and Xu, C. (2017). Convolutional neural networks for hyperspectral image classification. *Neurocomputing*, 219:88–98.

[39]. Bailer, C.; Habtegebrial, T.; Varanasi, K.; Stricker, D. Fast Feature Extraction with CNNs with Pooling Layers. *arXiv* 2018

[40]. Scherer, Dominik; Müller, Andreas C.; Behnke, Sven (2010). "Evaluation of Pooling Operations in Convolutional Architectures for Object Recognition" Artificial Neural Networks (ICANN), 20th International Conference on. Thessaloniki, Greece: Springer. pp. 92–101

[41]. Powers, David M W (2011). "Evaluation: From Precision, Recall and F-Measure to ROC, Informedness, Markedness & Correlation" (Journal of Machine Learning Technologies. 2 (1): 37–63.

[42]. Junge, M. R. J. and Dettori, J. R. (2018). Roc solid: Receiver operator characteristic (roc) curves as a foundation for better diagnostic tests. Global Spine Journal, 8(4):424–429.

[43]. Hanley, James A.; McNeil, Barbara J. (1983-09-01). "A method of comparing the areas under receiver operating characteristic curves derived from the same cases". Radiology. 148 (3): 839–843.

[44]. Sasaki, Y. (2007). "The truth of the F-measure".

[45]. Thi Kieu Khanh Ho, Jeonghwan Gwak, Om Prakash, Jong-In Song, and Chang Min Park "Utilizing Pretrained Deep Learning Models for Automated Pulmonary Tuberculosis Detection Using Chest Radiography". Springer Link (2019).

[46]. He, Kaiming; Zhang, Xiangyu; Ren, Shaoqing; Sun, Jian (He, Kaiming; Zhang, Xiangyu; Ren, Shaoqing; Sun, Jian (2015-12-10). "Deep Residual Learning for Image Recognition".

[47]. Szegedy, Christian, Sergey Ioffe, Vincent Vanhoucke, and Alexander A. Alemi. "Inception-v4, Inception-ResNet and the Impact of Residual Connections on Learning." In AAAI, vol. 4, p. 12. 2017.